U.S. Geological Survey.

[Reports. Open file]

Solution of the Gamma-Ray Transport Equation for Two Media, the Ground Source and Air, in Airborne Radioactivity Surveying.

by

Sakakura, A. Y.

A Y SAKAKURA

by A. Y. Sakakura

[illegible]

ILLUSTRATIONS

SOLUTION OF THE GAMMA-RAY TRANSPORT EQUATION FOR TWO MEDIA, THE GROUND SOURCE AND AIR, IN AIRBORNE RADIOACTIVITY SURVEYING.

INTRODUCTION

As the gamma-ray flux measured in airborne radioactivity surveying comes predominantly from a ground source essentially both infinitely thick and extensive for the radiation in question, a detailed solution of the steady state transport equation for gamma rays would be both interesting and useful. Such a solution for the two media, the ground source and air, would provide both the angular and spectral distribution of the gamma-ray flux from the uranium, thorium, and potassium series, and would establish the true total flux in air at various distances from the source.

Two methods of solution are available: the moments method of Spencer and Fano (1951), and the direct integration method of Keller and Heller (1955). The first method has been used with great success, and extensive series of calculations have been performed for one medium by Goldstein and Wilkins (1954). The second method, the direct numerical integration of the steady-state transport equation for neutrons with elastic scattering and an isotropic source (linearized Boltzmann), has also been successfully tested; this method shows that "small" errors introduced at the boundaries influence the solution only by a "small" amount, and that by taking a sufficiently fine mesh the numerical solution can be made as close as desired to the true transport solution.

[illegible] media involved; the air in which the [illegible] would be known at [illegible] distance from the ground surface, the ground in which the gamma-emitting sources are isotropically distributed [illegible]. The angular distribution of the flux was needed. [illegible] analogous neutron problem had already been programmed for the Univac computer, and modification of the neutron code necessary for the gamma-ray problem would be simple.

The first reason is more apparent than real as in the range where the Compton scatter effect dominates, the two-media problem can be cast into an equivalent one-medium problem. Although this is not possible in the low energy region, the flux in this region would be quite sensitive to the nature of the source material; consequently, one might as well proceed with an equivalent one-medium problem. After computing several problems within the overall problem, it became apparent that the second reason was no longer valid. In the low energy region, the flux in air at 500 feet from the air-source interface is approximately isotropic, and two or three Legendre moments are sufficient to characterize the angular flux. In the higher energy region, removal of the once-collided term as was done by Certaine (1953) would insure the need of but a few moments.

A total of 11 problems were programmed and computed under the code designation, Ariel, at the AEC Computing Facility at New York University. These problems correspond to the primary spectrum of RaC, Th C'', and K^{40} at the initial energies of 2.42, 2.63, and 1.45 mev respectively. The primary RaC spectrum was that given by Mladjenovic and Hedgran (1954); the thorium spectrum was that determined by N. Lazar of the Oak Ridge National Laboratory.

The RaC and thorium spectrum were normalized to 1 primary [illegible]
The cross-sections were taken from White (1952) with coherent [illegible] cluded.

The ground source was taken to be silicon dioxide of density 2.[illegible] The interface between air and the ground source was taken to be sea-level. It should be noted that for ground sources of different densities, the solution will apply if the concentration of gamma-emitting isotopes were expressed in terms of disintegrations per gram. The change of the air-ground interface from sea level to any higher altitude would require adjusting distance from source to the equivalent air density at sea level. Although the effect of the "law of atmosphere" is small compared to other errors, it was included in the computations inasmuch as it was simple to do so.

The raw output of the computer is the angular flux at various energies and distances from the air-source interface. However, the computer print-out data are not included in this report because of exceedingly large volume, equivalent to many hundreds of pages. These data are available in the files of the Geological Survey, and those who are interested may make copies.

ACKNOWLEDGMENTS

We are grateful to E. Bromberg, Director of the AEC Computing Facility, Institute of Mathematical Sciences, New York University, for the hospitality extended to Sakakura during his protracted stay at the Institute. We are particularly indebted to J. Heller of the Institute for modifying the Achilles code for integration of the neutron transport equation to the Ariel code for the gamma-ray transport equation, for his continued support in the debugging process, and for his overseeing the running of the problems on the computer. We thank N. Lamar of the Oak Ridge National Laboratory for determining the uranium and thorium spectra.

The work herein reported is part of an investigation carried on by the U. S. Geological Survey on behalf of the U. S. Atomic Energy Commission.

[illegible]

[illegible] numerical solutions [illegible] spherical geometries. We [illegible] the properties of the [illegible] equation appropriate to our problem; the general aspects are discussed thoroughly by Fano and by Goldstein and Wilkins. The Boltzmann equation is:

$$\left[z\frac{\partial}{\partial x} + \mu_a(\lambda) e^{-x/\ell} \right] Y(x,\lambda,z;\lambda_0) \tag{1}$$

$$= \int_{[\lambda_0,\lambda-2]} K_1(\lambda',\lambda) e^{-x/\ell} d\lambda' \int_{4\pi} d\Omega' \frac{\delta(\ldots -1-\lambda' \ldots)}{2\pi} Y(x,\lambda',z';\lambda_0), x > 0$$

$$\left[z\frac{\partial}{\partial x} + \mu_a(\lambda) \right] Y(x,\lambda,z;\lambda_0)$$

$$= \int_{[\lambda_0,\lambda-2]} K_1(\lambda',\lambda) d\lambda' \int_{4\pi} d\Omega' \frac{\delta(\ldots -1- \ldots)}{2\pi} Y(x,\lambda',z;\lambda_0) + \frac{1}{4\pi}\delta(\lambda-\lambda_0), x < 0$$

[illegible]

[illegible] unit vector [illegible] by the inclination to the x-axis, [illegible] x, [illegible]

λ = wave length, in Compton units, [illegible]

$$\lambda = \frac{0.511}{E}$$

$Y^1(x, \cdot, \cdot ; \lambda_0)$ = angular flux, the number of photons in wave-length

interval, $(\lambda, \lambda + d\lambda)$, in a solid angle, $d\vec{\Omega}$, [illegible]

normal to $\vec{u}$ per unit time due to a semi-infinite [illegible] source

emitting 1 photon of wave length, λ_0, per unit time per unit volume.

$e^{-x/\ell}$ = factor representing the "law of atmosphere"

$K_s(\lambda^1, \lambda)$ = linear differential Compton scattering cross-section from

λ^1 to λ for the source medium

$K_a(\lambda^1, \lambda)$ = linear differential Compton scattering from λ^1 to λ for

air at sea level density

$\mu_s(\lambda)$ = [illegible] attenuation [illegible]

photon of wave length, λ.

$\mu_a(\lambda)$ = linear total attenuation cross-section for air at sea level

density

$\lceil \lambda_0, \lambda - 2 \rceil$ = greater of the two λ's.

[illegible] geometry is depicted in Figure 1. To remove the delta (δ) function singularity, we write Y^1 as the sum of the unscattered flux and the scattered flux, Y:

$$Y^1(x,\lambda,z;\lambda_o) = Y(x,\lambda,z;\lambda_o) + \frac{\delta(\lambda-\lambda_o)}{4\pi\mu_s(\lambda_o)} f(x,z) \qquad (2)$$

where

$$f(x,z) = 1-e^{\frac{-\mu_s(\lambda_o)x}{z}} st(-z), \; x < 0 \qquad (3)$$

$$= \exp\left\{\frac{-\mu_s(\lambda_o)\ell(1-e^{-x/\ell})}{z}\right\} st(z), \; x > 0$$

Y, then, obeys the same transport equation (1) as Y^1 except that there is now a source term, S, in both media:

$$S_a(x,\lambda,z;\lambda_o) = \frac{K_a(\lambda_o,\lambda)e^{-x/\ell}}{4\pi\mu_s(\lambda_o)} \int_{4\pi} \frac{d\vec{u}^1\,\delta(\vec{u}\cdot\vec{u}^1-1-\lambda_o+\lambda)}{2\pi} f(x,z^1;\lambda_o), x > 0, \lambda-\lambda_o<2$$

$$S_s(x,\lambda,z;\lambda_o) = \frac{K_s(\lambda_o,\lambda)}{4\pi\mu_s(\lambda_o)} \int_{4\pi} \frac{d\vec{u}^1\,\delta(\vec{u}\cdot\vec{u}^1-1-\lambda_o+\lambda)}{2\pi} f(x,z^1;\lambda_o), x < 0, \; \lambda-\lambda_o< 2 \qquad (4)$$

$$= 0, \text{all } x \text{ and } \lambda-\lambda_o > 2$$

Now let

$$\ell = [illegible], \; x < 0$$

$$= [illegible](1-e^{-x[illegible]}), \; x > 0$$

then

$$K(x,\lambda,z;\lambda_o) = \int_{[\lambda_o,\lambda-2]}^{\lambda} K_s(\lambda^1,\lambda)\,d\lambda^1 \int_{4\pi} d\vec{u}^1 \frac{\delta(\vec{u}.\vec{u}^1-1-\lambda^1+\lambda)}{2\pi}\, Y(x,\lambda^1,z^1;\lambda_o),\ x < 0$$

$$= \int_{[\lambda_o,\lambda-2]}^{\lambda} K_a(\lambda^1,\lambda)\,d\lambda^1 \int_{4\pi} d\vec{u}^1 \frac{\delta(\vec{u}.\vec{u}^1-1-\lambda^1+\lambda)}{2\pi}\, Y(x,\lambda^1,z^1;\lambda_o),\ x > 0$$

and define

$$S(y,\lambda,z;\lambda_o) = S_a(x,\lambda,z;\lambda_o),\ x < 0$$
$$= S_b(x,\lambda,z;\lambda_o),\ x > 0$$

We change to discrete values of the wave-length, λ, and perform the integration by the trapezoidal rule, resulting in

$$z\frac{\partial Y}{\partial y}(x,\lambda_n,z;\lambda_o) + \sigma(\lambda_n)Y(x,\lambda_n,z;\lambda_o) = K^1(x,\lambda_n,z;\lambda_o) + S(x,\lambda_n,z;\lambda_o) \quad (5)$$

where

$$K^1(x,\lambda_n,z;\lambda_o) = K(x,\lambda_n,z;\lambda_o) - K(\lambda_n,\lambda_n)\frac{(\lambda_n-\lambda_{n-1})}{2}Y(x,\lambda_n,z;\lambda_o)$$

$$\sigma(\lambda_n) = \mu(\lambda_n) - K(\lambda_n,\lambda_n)\frac{(\lambda_n-\lambda_{n-1})}{2} = \mu(\lambda_n) - \frac{3}{8}\sigma_t(\lambda_n-\lambda_{n-1})$$

σ_t = Thompson cross-section

The right hand side no longer contains $Y(x,\lambda_n,z;\lambda_o)$, the unknown, and can thus be integrated:

$$Y(x\pm\delta x,\lambda_n,z;\lambda_o) = Y(x,\lambda_n,z;\lambda_o)\ \exp\left[\frac{-\delta y\sigma(\lambda n)}{z}\right] \quad (6)$$

$$+ \frac{1}{z}\int_y^{y+\delta y} \exp\left[\frac{-\sigma(\lambda n)(y+\delta y-y')}{z}\right]\left\{K^1(x^1,\lambda_n,z;\lambda_o) + S(x^1,\lambda_n,z;\lambda_o)\right\}dy^1,\ z \gtrless 0$$

where $\delta y(x) = y(x\pm\delta x) - y(x)$

[illegible] and takes the form

$$[illegible] \qquad (7)$$

[illegible]

$$[illegible] \; ; \; x < 0$$

$$[illegible] \; ; \; x > 0$$

[illegible]

$$K(x, \lambda_n, z; \lambda_c) = \frac{1 - [illegible]}{[illegible](\lambda_n)} - \frac{[illegible] - [illegible](\;)y - [illegible](\;)y}{[illegible](\lambda_n) - \frac{[illegible](\;)}{[illegible]}} \, st(-z), \quad x < 0$$

$$= \frac{\frac{-[illegible](\;)([illegible])}{[illegible]} - [illegible] - \frac{[illegible](\;)}{[illegible]} y}{[illegible](\lambda_n) - \frac{[illegible]}{[illegible]}} \, st(z^1), \quad x > 0 \qquad (8)$$

In order to integrate the collision term, $K(x, \lambda_n, z; \lambda_c)$ over y, it is necessary to use the discrete variable, x_k, rather than the continuous, x. We define, $x_{k+1} = x_k + \delta x$ and $y_k = y(x_k)$, and interpolate:

$$K^1(x^1, \lambda_n, z; \lambda_c) \sim - K^1(x_k, \lambda_n z; \lambda_c)\frac{(y - y_k - \delta y_k)}{\delta y_k} + K^1(x_k + \delta x, \lambda_n, z; \lambda_c)\frac{(y - y_k)}{\delta y_k} \qquad (9)$$

[illegible] (10) [illegible]:

$$[illegible] \qquad (10)$$

$$+ \frac{1}{\sigma(\lambda_n)} \left\{ [illegible] \right\} K'(x_k \pm \Delta x, \lambda_n, z; \lambda_0)$$

$$A(x_k, \lambda_n, z; \lambda_0)\, K'(x_k, \lambda_n, z; \lambda_0) + [illegible]$$

The transport equation thus takes the form

$$Y(x_k \pm \Delta x, \lambda_n, z; \lambda_0) \qquad (11)$$

$$[illegible] + T(x_k, \lambda_n, z; \lambda_0)$$

to which [illegible] method [illegible] can be readily applied, if the present infinite boundaries can be replaced by finite ones. This has been accomplished by assuming that the air is bounded on the right at 1000 feet by vacuum which makes the incoming flux zero at that point, and that the left hand boundary within the source is established by [illegible] rather than the incoming flux [illegible]. Now, [illegible] method can be directly applied, starting at the right hand boundary with [illegible] incoming flux, turning at the left hand boundary with [illegible] flux, and back to the right hand boundary.

Finally, in order to carry out the angular integration, we take J discrete values of [illegible]. Consider the integral

$$\int_{4\pi} d\vec{u}' \; \frac{\delta(\vec{u}\cdot\vec{u}' - 1 - [\text{illegible}]_{n})}{[\text{illegible}]} \; L(z') = I(z,\lambda_n,\lambda_{n'}) \tag{12}$$

where $L(z')$ is a function of z'. (In $T(x,\lambda_n,z;\lambda_c)$, $L(z') = g(x,z',z;\lambda_c)$, $n' < n$.) The integration over the azimuthal angle can be readily performed:

$$I(z,\lambda_n,\lambda_{n'}) = \frac{1}{\pi} \int_{\alpha}^{\beta} \frac{L(z')\; dz'}{\sqrt{(\beta - z')(z' - \alpha)}} \tag{13}$$

Where [illegible] $= 1 + \lambda_{n'} - \lambda_n$

[illegible] $+ \sqrt{(1-\quad)(\quad-\quad)}$ [illegible]

[illegible] $- \sqrt{(1-\quad)(1-\quad)}$ [illegible]

[illegible] function, $L(\ )$, is a linear combination [illegible]

$$L_1(z^1) + L_2(z^1)\, st(z^1 - z_m),$$

where L_1 and L_2 are well-behaved functions of z^1, [illegible] which may be [illegible].

(For example, in the source term we can write [illegible] $(-$ [illegible] $) = 1-$ [illegible]. Here

$z_m = 0$.) Integration is performed by the [illegible] of [illegible]. The integral

involving $L_1(z^1)$ is readily performed:

$$\frac{1}{\pi}\int_{\alpha}^{\beta} \frac{L_1(z^1)}{\sqrt{(\beta-z^1)(z^1-\alpha)}}\,dz^1 = \frac{2}{J}\sum_{p=0}^{J/2} L_1(z^1{}_p), \qquad z^1{}_p = \frac{\beta-\alpha}{2}\,O_p + \frac{\beta+\alpha}{2} \quad (14)$$

where O_p's are the roots of Tschebyscheff polynomial of degree $J/2$.

The integral involving the step function is:

$$\frac{1}{\pi}\int_{\alpha}^{\beta} \frac{L_2(z^1)\, st(z^1 - z_m)}{\sqrt{(\beta-z^1)(z^1-\alpha)}}\,dz^1 = 0 \qquad \beta < z_m \quad (15)$$

$$= \frac{2}{J}\sum_{p=0}^{J/2} L_2(z^1{}_p)\sqrt{\frac{z_p - z_m}{z_p - \alpha}}, \quad \beta > z_m > \alpha$$

$$z^1{}_p = \frac{\beta - z_m}{2}\,O_p + \frac{\beta + z_m}{2}$$

and is identical to (14) for $\alpha \le z_m$. For the source terms, the L's can be

evaluated at z_p; for the K^1's, the Y's are linearly interpolated between

two z's bracketing z_p, i.e.

$$Y(x_k, \lambda_{n^1}, z_p) \sim Y(x_k, \lambda_{n^1}, z_q)\frac{(z_p - z_{q-1})}{\delta_z} + Y(x_k, \lambda_{n^1}, z_{q-1})\frac{(z_q - z_p)}{\delta_z} \quad (16)$$

$$\text{where} \qquad \delta_z = \frac{2}{J-1}, \quad z_q = \delta_z + z_{q-1}$$

[illegible] appears in K' is introduced [illegible] steps, which [illegible] the number of collisions [illegible] to reach a given energy, [illegible] a restriction on the values [illegible] for the energies close to the initial energy. The use of z_m insures that the numerical integration is restricted to the significant portion of the angular interval.

In actual running of the problem, the following parameters were used:

δx_s = .05 ft. δx_a = 100 ft. δ [illegible]

The thickness of air (to the right boundary) was taken to be 1000 feet; and the thickness of the source (to the left boundary) to be 5 mean free paths of the primary photon.

To determine the independence of the results to the choice in parameters, we have run a problem with the following parameters:

δx_s = .05 ft. δx_a = 50 ft. δ [illegible]

The thickness of the air was taken to be 1000 feet; and the thickness of the source to be 7 mean free paths. Taking the initial energy to be 2.63 mev, the flux at 1.76 mev, which was separated from 2.63 mev by 5 intermediate energies instead of the usual two, was examined. As the flux within the source would be little influenced by the change of parameters in air, the differences in the two problems would show the effect of the change in δz, δx, and δ [illegible]. Throughout the [illegible] and at the boundary, the fluxes for the two problems differ by less than one percent, and we thus conclude that the δz, δx, and δ [illegible] used are adequate for the source media. As the flux in air at $z = 1$ is [illegible] the boundary imposed on the [illegible] of the effect of change in δx_c. [illegible] two problems, even at [illegible] feet the differences were less than [illegible] percent, indicating that δx_c = 100 feet is sufficiently fine mesh.

Because of the sharply forward peaked nature of the high energy fluxes, the evaluation of the source terms depends strongly on the choice of [illegible] when [illegible] 0. The angular fluxes differ about five percent in the range 1>z>0.1, about ten percent in the range 0.1>z>0, and about an order of [illegible] may be [illegible]. However, this error is not important as the flux in the backward direction is very small compared to the forward flux. Thus, the major contribution to the backward fluxes at energies close to the source energies ([illegible]) is the scattering from the forward fluxes. At lower energies, the backward flux is of the same order of magnitude as the forward flux, and the major contribution is the scattering from higher energy backward fluxes which in turn come from scattering of high energy forward fluxes. Thus, the effect of source term inaccuracy and position of the right hand boundary on the backward flux is not serious at low energies whereas at high energies, the backward flux itself is not important. The accuracy of the Legendre moments is good, the difference being five percent at 1000 feet and two percent at 500 feet.

Discussion of general results

Following Goldstein and Wilkins (1954), we call $Y_o(x,\lambda)$ the flux, as contrasted to the angular flux $Y(x,\lambda,z)$, to which it is related by:

$$Y_o(x,\lambda) = \int_{4\pi} d\vec{\mu}\, Y(x,\lambda,z) \tag{1}$$

The flux, divided by the velocity of light, is the total number of photons of wavelength λ, regardless of direction of travel, contained in a unit volume. We also introduce the spectral flux, $N(x,E)$ which is related to the flux by :

$$N(x,E) = -\frac{d\lambda}{dE} Y_o(x,\lambda) = \frac{0.\text{[illegible]}}{\lambda^2} Y_o(x,\lambda) \tag{2}$$

which gives the total number of photons/unit area/sec. regardless of direction in the energy interval dE. They are related to the integral flux

$$Y_c(x,\lambda) = N_c(x,E) = \int_E^{E_o} N(x,E)\,dE^1 = \int_{\lambda_o}^{\lambda} Y_o(x,\lambda^1)\,d\lambda^1 \tag{3}$$

The total integral flux is

$$Y_c{}^1(x,\lambda) = N_c^1(x,E) = N_c(x,E) + \text{primary}.$$

We also define the Legendre moments, $\psi_\ell(x,\lambda)$:

$$\psi_\ell(x,\lambda) = \frac{2\ell+1}{4\pi} \int_{-1}^{+1} Y_o(x,\lambda,z) P_\ell(z)\, d\vec{\mu} \tag{4}$$

where $P_\ell(z)$ is Legendre polynomial of order ℓ.

Note that ψ_o for a given source is Y_o of a source $\frac{1}{4\pi}$ times as intense.

[illegible]

[illegible] the initial energy. [illegible]

[illegible] where the primed quantities are [illegible] computed by the

[illegible]. The third and fourth order moments are good to a factor

of 2, the second order moment is good to ten percent, and the first and zero

order moments are good to five percent. As strong angular dependences are

characteristic of energies near the initial energy, it is expected that the

moments would be more accurate at lower energies.

In table 2 we have plotted the reconstructed flux

$$\phi^L(x,\lambda,z) = \sum_{\ell=0}^{L} \phi_\ell(x,\lambda)P_\ell(z)$$

in the column labeled by various values of L for x=0, 500, and 1,000 feet

for various wave lengths. The $\pm$ sign on $\lambda = 2.211$ refers to the values of

the flux before and after the first scattered flux vanishes. Note that at

500 feet at lower energies, L = 2 approximation gives results within three

percent of the true flux, labeled Ariel, except in the neighborhood of [illegible] -1. [illegible] [illegible], [illegible] ([illegible]) for the plane mono-directional source, agreement for the [illegible] energies [illegible] good. The reason the fourth moment [illegible] than the third moment is [illegible].

We finally compare (in table [illegible]) the [illegible] build-up factor from 2.43 to 0.4 mev, computed from Nuclear Development Associates [illegible] (Goldstein and Wilkins, 1954) in a manner outlined in a previous paper (Sakakura, 1957), with the build-up computed from the [illegible]. The results are in reasonable agreement. Note that the [illegible] build-up [illegible] are lower than the moments build-up factor, [illegible] because of finite thickness of air.

In figure [illegible] we have plotted the [illegible] at various energies [illegible] to source energies of 2.63, 1.4[illegible], and 0.[illegible] mev. [illegible] isotropicity at E = 0.2 mev. for the sources of [illegible] mev energy, whereas the one due to the source of 0.[illegible] mev. is much more anisotropic. Note also the fact that at $\lambda > \lambda_0 + [illegible]$ the fluxes are roughly equal regardless of the initial energy due to the photons forgetting their initial energy after many collisions. At E = 0.39 mev, for which $\lambda << \lambda_0 + 2$ for all thr[illegible]

[illegible] produced [illegible] the 0.[illegible] mev source.

The angular flux at E = 0.1 and 0.0[illegible] mev are shown for the 2.63 mev source—the angular flux [illegible] the other two sources should not differ [illegible] from this.

In Figure 3, we have plotted the angular flux at $\mu = 1$, $Y(x,\lambda,1)$, as a function of distance in air at E = 2.42 mev, and E = 0.2 mev due to sources of 2.63 mev energy. The solid line represents what the flux would be if the air were purely absorptive. The contribution from air scattering even at energies close to the source energy and in the extreme forward direction is quite significant.

In figure 4 are plotted the angular fluxes in the backward directions, $\mu = -1, -\frac{1}{\sqrt{3}}$, and at low energies, E = 0.[illegible] [illegible] mev, due to a source of [illegible] mev. [illegible] the [illegible] independence of the flux to x and [illegible]. [illegible] is approximately exponential with absorption [illegible] of the ratio,

[illegible]

i.e., the [illegible] of the angular flux [illegible] in the forward direction, at $z = 0$ and [illegible]

at low energy, [illegible]

Thus, [illegible]

[illegible] is:

1. approximately isotropic

2. approximately independent of direction and energy in the backward direction

3. attenuated with the absorption coefficient of the source energy

4. independent of source energy.

Further, even at high energy, the contribution in the forward direction from scattering is considerable.

[illegible] Only when the electronic density of the detector [illegible] approximately [illegible] to that of [illegible] in which it is immersed, or when the dimension of the detector system is small fraction of the mean free paths of the [illegible] in the detector, is the [illegible] flux equal to the flux in the absence of the detector system.

[illegible] are [illegible] not met by airborne radiation detectors as they are usually [illegible] to minimize cosmic ray background from above and from the sides. However, as the forward flux is little distorted by the presence of the detector, we can use the undisturbed flux at the detector as an apparent surface source density, i.e., consider figure 6 which depicts a typical detector arrangement. We then [illegible] the undisturbed forward flux at x, as having an effective surface [illegible] (x, λ, t), in photons/unit area/ [illegible] the effect of this flux on the [illegible]

To see the difference between [illegible] and the actual response of a shielded radiation detector, consider a 100 per cent efficient detector which receives all forward fluxes but none in the backward direction. This can be thought of as a thick crystal detector of large lateral extent so that the edge effects are unimportant, and heavily shielded in the back. Then the count rate is simply $C(x,\lambda) = \int$ [illegible] (x,λ,Ω) which we may call the current. In figure [illegible] we have compared the count rate, $C(x,\lambda)$, and the flux, $I(x,\lambda)$, [illegible] due to a radium C source emitting [illegible] /sec. [illegible]; the flux is identical to equilibrium uranium [illegible] for energies above 0.[illegible] mev. Curves one and two are the primary flux and current respectively due to the 0.609 mev gamma ray; as each curve is multiplied by a delta function, they are actually not comparable to the other curves in figure 1. These two curves may be thought of as representing the flux and current in the small interval λ_0 to $\lambda_0 + \delta\lambda$. In any event, it is evident that there is a large difference between the fluxes and the currents near the interface of source and air. With increasing distance from the source, the distance dependence of curves 1 and 2 decreases as much as some isotropy is attained. The sharp drop in the fluxes (curves 3 and 5 in figure 7) near 1000 feet is not real as this drop is induced by the imposed boundary condition at 1000 feet.

The quantity measured by a radiation detector is dependent on the spectral energy and angular response of the detector, and is not the total flux but only a portion of the flux. Nevertheless, examination of the total flux characteristics should yield some important conclusions bearing on gamma measurements at considerable air distances from a source.

Figures 8, 9, and 10 display the total integral fluxes due to RaC, thorium, and K^{40} sources. The RaC source is normalized to $\frac{1}{4\pi}$ gamma rays/ft.^{3}/sec., the thorium source to $\frac{1}{4\pi}$ disintegrations/ft.^{3}/sec., and K^{40} source to $\frac{1}{4\pi}$ gamma rays/ft.^{3}/sec. The dashed line curves denote the integral flux due solely to the unscattered photons. It is evident that the scattered flux forms the major part of the integral flux.

We can estimate the relative importance of Ra B to the integral flux from 2.4 mev. to 0.2 mev. The total integral flux at 500 feet from the source E_0 to 0.2 mev., [illegible] $\frac{1}{4\pi}$ gamma rays/ft.^{2}/sec. of energies 0.354, 0.297, and 0.243 were found to be .00063, .00053, and .00041 photons/ft.^{2}/sec. If we use the absolute intensity of the 2.2 mev. gamma ray estimated by Ellis and Aston (1930) and use Mladjenevic and Hedgran's (1954) values of the relative intensities of the RaC gamma rays, we find that RaC emits about 1.42 primary gammas/disintegration. RaB emits 3 gamma rays of 0.354, 0.297, and 0.243 mev energies at the rate of 0.45, 0.258, and 0.115 gamma/disintegration (Ellis and Aston, 1930). Then the additional flux at 500 feet contributed by RaB is

$$\frac{(0.45 \times .00063) + (0.258 \times .00053) + (0.115 \times .00041)}{1.42} = 0.00033$$

photons/ft.^{2}/sec.

or $\frac{.00033}{.007} \times 100 \sim 5$ percent additional flux. Thus, the contribution of RaB to the total flux is negligible.

[illegible] radium and its [illegible] E_0 < 0.2 mev. For the [illegible] assume [illegible] ray of 0.2 mev is emitted [illegible] Let us assume we [illegible] contribution to the integral [illegible] in the range 0.2 mev [illegible] by this gamma ray is

$$\text{Primary flux} = \frac{1}{8\mu_s(\ldots)} E_2(\mu_s(\ldots)x)$$

$$\text{where } E_2(p) = \int_1^{\infty} \frac{e^{-pt}}{t^2}\,dt$$

the [illegible] order exponential integral. When the flux is evaluated at x = 500 feet, and E_0 = 0.2 mev (λ_i = 2.551), it is found to be 1.2 × 10^{-4} photons/ft.^{2}/sec. The contribution to the integral flux in the range 0.2 mev ± 10 percent due to scattering from higher energy gamma rays is

$$\int_{0.18}^{0.22} N_s(x,E)dE = N_0(x,0.18)-N_0(x,0.22), \sim 0.92 \times 10^{-3} \text{ photons/ft.}^2\text{/sec.}$$

Taking into account the number of gamma rays per disintegration, we find that [illegible] line yield 100 × [illegible] [illegible] percent of the flux in the [illegible] energy region 0.2 mev ± 10 percent. Considering the instability [illegible], it would [illegible] difficult to detect such a line. It seems highly unlikely that spectral energy measurements at considerable air distances from a source could discriminate variations in equilibrium among the precursors of radium in the uranium series.

It is beyond the scope of this report to point out and to develop fully all possible applications of these particular solutions of the gamma-ray transport equation. A few possible uses are:

1. Establishment of the true total flux for various source concentrations, for the uranium, thorium, and potassium series, both individually and combined in varying amounts.

2. Comparison of the total flux, $Y(x,\lambda)$, to the observed, count-rate flux, $C(x,\lambda)$, for a particular technique of measurement.

3. Extension of the solutions to gamma-ray measurements at the ground surface and within the source (gamma-ray logging).

4. Evaluation of the possibility of spectral energy discrimination to determine the relative contributions from the uranium, thorium, and potassium series.

References cited.

1. Fano, U., 1953, Penetration of X- and gamma rays to extremely great depths: U. S. Nat. Bur. Standards Jour. Research, v. 51, no. 2, p. 95-121.

2. Goldstein, H., and Wilkins, J. E., 1954, Calculations of the penetration of gamma rays, final report: U. S. Atomic Energy Comm. NYO-3075, ussued by U. S. Atomic Energy Comm. Tech. Inf. Service, Oak Ridge, Tenn.

3. Keller, H. B., and Heller, J., 1955, On the numerical integration of the neutron transport equation: U. S. Atomic Energy Comm. NYO-6481.

4. Mladjenevic, M., and Hedgran, A., 1954, An investigation of the Compton secondaries from RaC gamma rays: Arkiv für Fysik, Band 8, Hafte 4, p. 49-63.

5. Ellis, C. D., and Aston, G. H., Proc. Rag. Soc. A129, 180, (1930).

6. Sakakura, A. Y., 1957, Scattered gamma rays from thick uranium sources, U. S. Geol. Survey Bull. 1052-A.

7. Certaine, J., 1953, Angular distribution of photons from plane mono-energetic sources, U. S. Atomic Energy Comm. NYO-3074, N.D.A. report 15C-10, contract AT(30-1)862.

Lazar, ~~Oak Ridge Nat. Lab.,~~

8. ~~Lazar, N. H., private communication, 1955.~~

9. White, G. R., X-ray attenuation coefficients from 10 kev. to 100 mev.: N.B.S. report 1003, May 13, 1952.

10. Spencer, L. V., and Fano, U., J. Res. N.B.S. 46, 446 (1951).

Table: Accuracy of Legendre Moments

Table 4. **Accuracy of the Legendre Moments**

Moments:	[illegible] feet	[illegible] feet	[illegible] feet
ψ_0 ψ_0' $(\psi_0-\psi_0')/\psi_0$	0.0[illegible]3 0.0[illegible]9 0.0[illegible]6	0.0[illegible]0 0.0[illegible] - .0[illegible]	0.0[illegible] 0.0[illegible] - .0[illegible]
ψ_1 ψ_1' $(\psi_1-\psi_1')/\psi_1$	0.0[illegible] 0.0[illegible]5 - .0[illegible]3	0.0[illegible] 0.0[illegible]0 - .0[illegible]6	0.0[illegible]3 0.0[illegible]6 - .0[illegible]
ψ_2 ψ_2' $(\psi_2-\psi_2')/\psi_2$	0.0 .00795 ———	0.0[illegible]3 0.0[illegible]5 - .073	0.0[illegible] 0.0[illegible] - .0[illegible]
ψ_3 ψ_3' $(\psi_3-\psi_3')/\psi_3$	- .0[illegible]3 - .0[illegible]3 0.[illegible]	- .00[illegible]3 - .00[illegible]6 0.[illegible]	0.00[illegible] 0.0[illegible] -0.[illegible]
ψ_4 ψ_4' $(\psi_4-\psi_4')/\psi_4$	0.0 0.00[illegible]3 ———	- .0[illegible] - .00757 0.[illegible]	- .00[illegible] 0.00[illegible]0 -1.[illegible]

TABLE 2

71

32

L = [illegible], z		0	1	2	3	4	Axial
X=0°	1	.04978	.1264	.1348	.09811	.1036	0.1046
	9/11	.04978	.1111	.1188	.1127	.1118	0.1046
	7/11	.04978	.09907	.1057	.1126	.1102	0.1046
	5/11	.04978	.08568	.08809	.1018	.1000	0.1046
	3/11	.04978	.07134	.06885	.08196	.08868	0.1046
	1/11	.04978	.05707	.05319	.06574	.06068	0.1046
	-1/11	.04978	.04288	.03898	.03378	.04568	0
	-3/11	.04978	.02882	.02565	.02173	.02540	0
	-5/11	.04978	.01457	.01276	-.003166	-.008924	0
	-7/11	.04978	.0000008154	.0005540	-.01101	-.01137	0
	-9/11	.04978	-.01487	-.01086	-.006823	-.005790	0
	-1	.04978	-.02863	-.02058	.02768	.02381	0

L = [illegible], z		0	1	2	3	4	Axial
X=[illegible]°	1	.08514	.07616	.1077	.1083	.1088	.0873
	9/11	.08514	.06649	.08379	.09382	.08456	.0821
	7/11	.08514	.05701	.06110	.06128	.06415	.0712
	5/11	.08514	.04433	.04821	.04138	.04377	.0544
	3/11	.08514	.03965	.02841	.02465	.02546	.0360
	1/11	.08514	.02978	.01391	.01396	.01135	.00886
	-1/11	.08514	.02090	.004404	.005576	.001970	0
	-3/11	.08514	.01182	-.001428	-.001540	.000471	0
	-5/11	.08514	.001843	-.004843	-.004416	.000803	0
	-7/11	.08514	-.007138	-.003837	-.003957	-.0007311	0
	-9/11	.08514	-.01462	-.0008035	-.0004407	.001175	0
	-1	.08514	-.02549	.004468	.007044	-.0006263	0

L = [illegible], z		0	1	2	3	4	Axial
X=[illegible]°	1	.01883	.03977	[illegible]	.07312	.07773	.05948
	9/11	.01883	[illegible]	.04711	[illegible]	[illegible]	[illegible]
	7/11	.01883	[illegible]	.02879	[illegible]	[illegible]	.03476
	5/11	.01883	[illegible]	[illegible]	[illegible]	.01449	.02770
	3/11	.01883	[illegible]	[illegible]	[illegible]	[illegible]	.00911
	1/11	.01883	[illegible]	[illegible]	[illegible]	[illegible]	[illegible]
	-1/11	.01883	[illegible]	[illegible]	[illegible]	[illegible]	0
	-3/11	.01883	[illegible]	[illegible]	[illegible]	[illegible]	0
	-5/11	.01883	[illegible]	[illegible]	[illegible]	[illegible]	0
	-7/11	.01883	[illegible]	[illegible]	[illegible]	[illegible]	0
	-9/11	.01883	[illegible]	[illegible]	[illegible]	[illegible]	0
	-1						

Table 2 (cont'd)

X	y/L	0	1	2	3	4	Trial
X=0'	1	.009108	.01918	.01968	.01995	.02728	.02441
	9/11	.009108	.01735	.01760	.01764	.02356	.01718
	7/11	.009108	.01552	.01557	.01549	.01450	.01557
	5/11	.009108	.01369	.01359	.01347	.01298	.01396
	3/11	.009108	.01186	.01166	.01157	.01185	.01195
	1/11	.009108	.01002	.009779	.009761	.01055	.01034
	-1/11	.009108	.008192	.007967	.007978	.008736	.007860
	-3/11	.009108	.006360	.006165	.006259	.006540	.005824
	-5/11	.009108	.004528	.004433	.004551	.004054	.004190
	-7/11	.009108	.002696	.002750	.002932	.001838	.002640
	-9/11	.009108	.0008644	.001118	.001080	.0006777	.001171
	-1	.009108	-.0009674	-.0001651	-.0007724	.001604	.0000591

X	y/L	0	1	2	3	4	Trial
X=500'	1	.003884	.009703	.01240	.01431	.01657	.01282
	9/11	.003884	.008645	.01000	.01088	.009985	.0101
	7/11	.003884	.007587	.007876	.007276	.006321	.007200
	5/11	.003984	.006529	.006016	.005192	.004670	.005422
	3/11	.003884	.005471	.004474	.003733	.004003	.004449
	1/11	.003884	.004413	.003098	.002939	.003612	.003807
	-1/11	.003884	.003355	.002040	.002300	.003073	.002757
	-3/11	.003884	.002297	.001250	.001941	.002211	.001846
	-5/11	.003884	.001239	.0007265	.001588	.001110	.001132
	-7/11	.003884	.0001810	.0004707	.001069	.0002121	.0005299
	-9/11	.003884	-.0008769	.0004822	.0002084	-.0001842	.0001703
	-1	.003884	-.001935	.0007611	.001167	.001079	.0000473

X	y/L	0	1	2	3	4	Trial
X=1000'	1	.001708	.005017	.007085	.007837	.008535	[illegible]
	9/11	.001708	.004415	.004848	.005529	.005372	.005379
	7/11	.001708	.003814	.004034	.003856	.003474	.003695
	5/11	.001708	.003212	.002823	.002567	.002376	.002753
	3/11	.001708	.002611	.001815	.001610	.001728	.002083
	1/11	.001708	.002009	.001010	.0009333	.001243	.001502
	-1/11	.001708	.001407	.0004066	.0004895	.0007548	0
	-3/11	.001708	.0008059	.00001071	.0002151	.0003738	0
	-5/11	.001708	.0002043	-.0001890	.00007055	-.0001208	0
	-7/11	.001708	-.0003972	-.0001771	[illegible]	-.0003875	0
	-9/11	.001708	-.0009987	.00003391	-.0004728	-.0007043	0
	-1	.001708	-.001600	.0004481	-.0001236	.0007764	0

Table 2 (contd)

	L	0	1	2	3	4	Axial
I=0'	1	.006878	.007352	.007952	.007903	.009621	.007619
	9/11	.006878	.007264	.007267	.007417	.007116	.007887
	7/11	.006878	.007180	.007202	.007092	.006360	.007152
	5/11	.006878	.007094	.007092	.006899	.006533	.007008
	3/11	.006878	.007009	.006930	.006804	.007011	.006860
	1/11	.006878	.006921	.006824	.006777	.007366	.006638
	-1/11	.006878	.006835	.006738	.006755	.007377	.007896
	-3/11	.006878	.006749	.006672	. 06798	.007004	.006963
	-5/11	.006878	.006663	.006605	.006787	.006416.	.006767
	-7/11	.006878	.006577	.006538	.006707	.005975	.006599
	-9/11	.006878	.006491	.006591	.006942	.006241	.006393
	-1	.006878	.006405	.006604	.006253	.007971	[illegible]

	L	0	1	2	3	4	Axial
I=500'	1	.002784	.003137	.003890	.004078	.004787	.003718
	9/11	.002784	.003073	.003453	.003400	.003363	.003408
	7/11	.002784	.003010	.003092	.003037	.002768	.003093
	5/11	.002784	.002946	.002803	.002719	.002577	[illegible]
	3/11	.002784	.002883	.002550	.002523	.002603	[illegible]
	1/11	.002784	.002819	.002457	.002427	.002657	[illegible]
	-1/11	.002784	.002756	.002309	[illegible]	[illegible]	.002309
	-3/11	.002784	[illegible]	.002400	.002467	[illegible]	[illegible]
	-5/11	.002784	.002629	.002465	.002570	.002437	.002630
	-7/11	.002784	.002565	[illegible]	.002704	.002419	.002767
	-9/11	.002784	[illegible]	.002681	[illegible]	.002738	.002803
	-1	.002784	.002438	. 03191	.003003	. 03678	.002817

	L	0	1	2	3	4	Axial
I=1000'	1	.0006184	.001670	.001979	.001775	.001933	.001720
	9/11	.0006184	.001479	.001445	.001613	.001585	.001595
	7/11	.0006184	.001288	.001373	.001391	.001325	.001136
	5/11	.0006184	.001096	.001016	.001134	.001101	.001185
	3/11	.0006184	.0009053	.0007773	.0008979	.008770	.001089
	1/11	.0006184	.0007140	.0005575	.0004937	.0004383	.0008676
	-1/11	.0006184	.0005278	.0003677	.0003390	.0003867	0
	-3/11	.0006184	.0003316	.0002037	.0001231	.0001479	0
	-5/11	.0006184	.0001404	.00007778	-.00007768	-.00005649	0
	-7/11	.0006184	-.00005083	-.00001545	-.00009217	-.0001528	0
	-9/11	.0006184	-.0002420	-.00007608	-.00004411	-.00007186	0
	-1	.0006184	-.0004333	-.0001039	.0001208	.0002795	0

Table 2 (cont'd)

z \ L =	0	1	2	3	4	Axial
1	.006029	.007079	.007227	.007266	.007782	.006933
9/11	.006029	.006888	.006963	.006968	.006703	.006806
7/11	.006029	.006697	.006713	.006701	.006055	.006679
5/11	.006029	.006506	.006478	.006461	.006138	.006544
3/11	.006029	.006315	.006298	.006244	.006426	.006384
1/11	.006029	.006124	.006057	.006047	.006569	.006203
-1/11	.006029	.005933	.005861	.005[illegible]7	.006389	.006080
-3/11	.006029	.005742	.005685	.005699	.005882	.005726
-5/11	.006029	.005552	.005573	.005541	.005218	.005520
-7/11	.006029	.005360	.005376	.005388	.004742	.005392
-9/11	.006029	.005160	.005244	.005238	.004973	.005258
-1	.006029	.004979	.005126	.005057	.006403	.004988

z \ L =	0	1	2	3	4	Axial
1	.002646	.003264	.003775	.004005	.004671	.003640
9/11	.002646	.003152	.003409	.003442	.003386	.003368
7/11	.002646	.003039	.003094	.003023	.002739	.002977
5/11	.002646	.002927	.002930	.002777	.002985	.002800
3/11	.002646	.002815	.002616	.002534	.002614	.002592
1/11	.002646	.002702	.002453	.002422	.002651	.002467
-1/11	.002646	.002590	.002361	.002371	.002602	.002388
-3/11	.002646	.002478	.002279	.002361	.002441	.002366
-5/11	.002646	.002365	.002268	.002370	.002779	.002387
-7/11	.002646	.002253	.002305	.002379	.003095	.002364
-9/11	.002646	.002141	.002398	.002366	.002749	.002317
-1	.002646	.002088	.002540	.002310	.002977	.002260

z \ L =	0	1	2	3	4	Axial
1	.0006178	.001668	.001995	.0017[illegible]	.001925	0.001713
9/11	.0006178	.001477	.001642	.001510	.001483	.001528
7/11	.0006178	.001256	.001321	.001392	.001325	.001335
5/11	.0006178	.001095	.001033	.001134	.001101	.001185
3/11	.0006178	.0009042	.0007771	.0005944	.0008777	.001029
1/11	.0006178	.0007133	.0005537	.0005842	.0006381	.0009613
-1/11	.0006178	.0005723	.0003627	.0003377	.0003561	0
-3/11	.0006178	.0003324	.0002043	.0001730	.0001415	0
-5/11	.0006178	.0001405	.00007927	-.00002317	-.00005690	0
-7/11	.0006179	-.00009044	-.00001528	-.00009568	-.0001524	0
-9/11	.0006178	-.0002414	-.00007637	-.0000415	-.00007151	0
-1	.0006179	-.0004373	-.0001090	.0001219	.0002784	0

Table 2 (Cont'd)

[illegible]	z \ L =	0	1	2	3	4	Axial
	1	.005333	[illegible]	[illegible]	.006466	.01064	.006162
	9/11	.005333	[illegible]	.006206	.006208	.003871	.006066
	7/11	.005333	[illegible]	.005971	[illegible]	.002701	[illegible]
	5/11	.005333	.005779	.005753	.005747	[illegible]	[illegible]
	3/11	.005333	[illegible]	.005547	.005542	.007151	.005665
	1/11	.005333	[illegible]	.005355	.005353	[illegible]	.005476
	-1/11	.005333	.004244	.005176	.005178	[illegible]	.005315
	-3/11	.005333	.005004	[illegible]	.005017	[illegible]	.005053
	-5/11	.005333	[illegible]	.004641	.004657	.002019	.004844
	-7/11	.005333	.004704	.004724	.004729	-.000[illegible]	.004465
	-9/11	.005333	.004531	.004601	.004509	.002261	.004527
	-1	.005333	.004352	.004498	.004477	.01705	.004397

[illegible]	z \ L =	0	1	2	3	4	Axial
	1	.002342	.003011	.003344	[illegible]	.004443	.003267
	9/11	.002342	.002981	.003044	.003113	.003003	.003035
	7/11	.002342	.002602	.002536	.002778	.002530	.002820
	5/11	.002342	.002642	.002617	.002559	[illegible]	.002618
	3/11	.002342	.002562	.002429	.002342	[illegible]	.002444
	1/11	.002342	.002442	.002275	.002278	.002471	.002312
	-1/11	.002342	.002322	.002155	.002173	.002369	
	-3/11	.002342	.002202	.002069	.002116	.002192	
	-5/11	.002342	.002082	.002017	.002075	.001941	
	-7/11	.002342	.001962	.001999	.002039	.001771	
	-9/11	.002342	.001842	.002015	.001996	.001[illegible]	
	-1	.002342	.001722	.002066	.001995	.002564	

[illegible]1000'	z \ L =	0	1	2	3	4	Axial
	1	.0005406	.001644	.001760	.001565	.001695	.001511
	9/11	.0005406	.001296	.001115	.001116	.001395	.001337
	7/11	.0005406	.001128	.001160	.001281	.001165	.001168
	5/11	.0005406	.0009604	.0009041	.0009912	.0009637	.001039
	3/11	.0005406	.0007985	.0006774	.0007473	.0007628	[illegible]
	1/11	.0005406	.0006246	.0004601	.0005064	.0005509	.0007366
	-1/11	.0005406	.0004567	.0003123	.0002660	.0001306	.0
	-3/11	.0005406	.0002888	.0001737	.0001039	.0001[illegible]	.0
	-5/11	.0005406	.0001209	.00006462	-.00008853	-.00005008	.0
	-7/11	.0005406	-.00001695	-.00001212	-.00007541	-.0001307	.0
	-9/11	.0005406	-.0002148	-.00007524	-.0000771	-.0006041	.0
	-1	.0005406	-.0003427	-.0000461	.0001085	.0005778	.0

Table 3. Comparison of Ariel and Moments methods.

X =	Moments	Ariel
0'	2.08	2.06
100'	2.41	2.31
300'	2.87	2.74
500'	3.51	3.11
700'	3.63	3.47

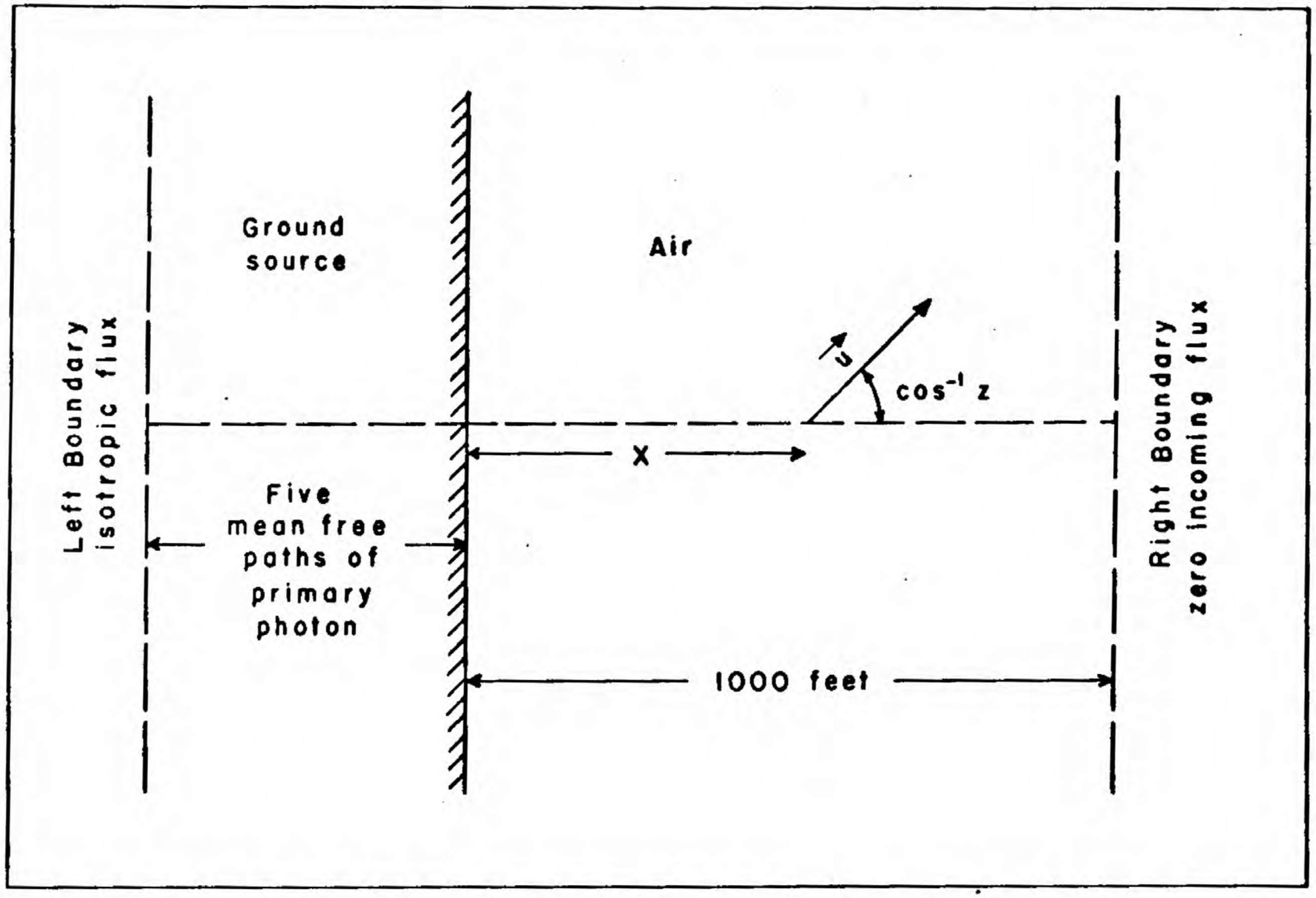

Figure 1- Geometry for two media, ground and air

Figure 2. Angular Flux, Y(500, λ, Z; λ_o).

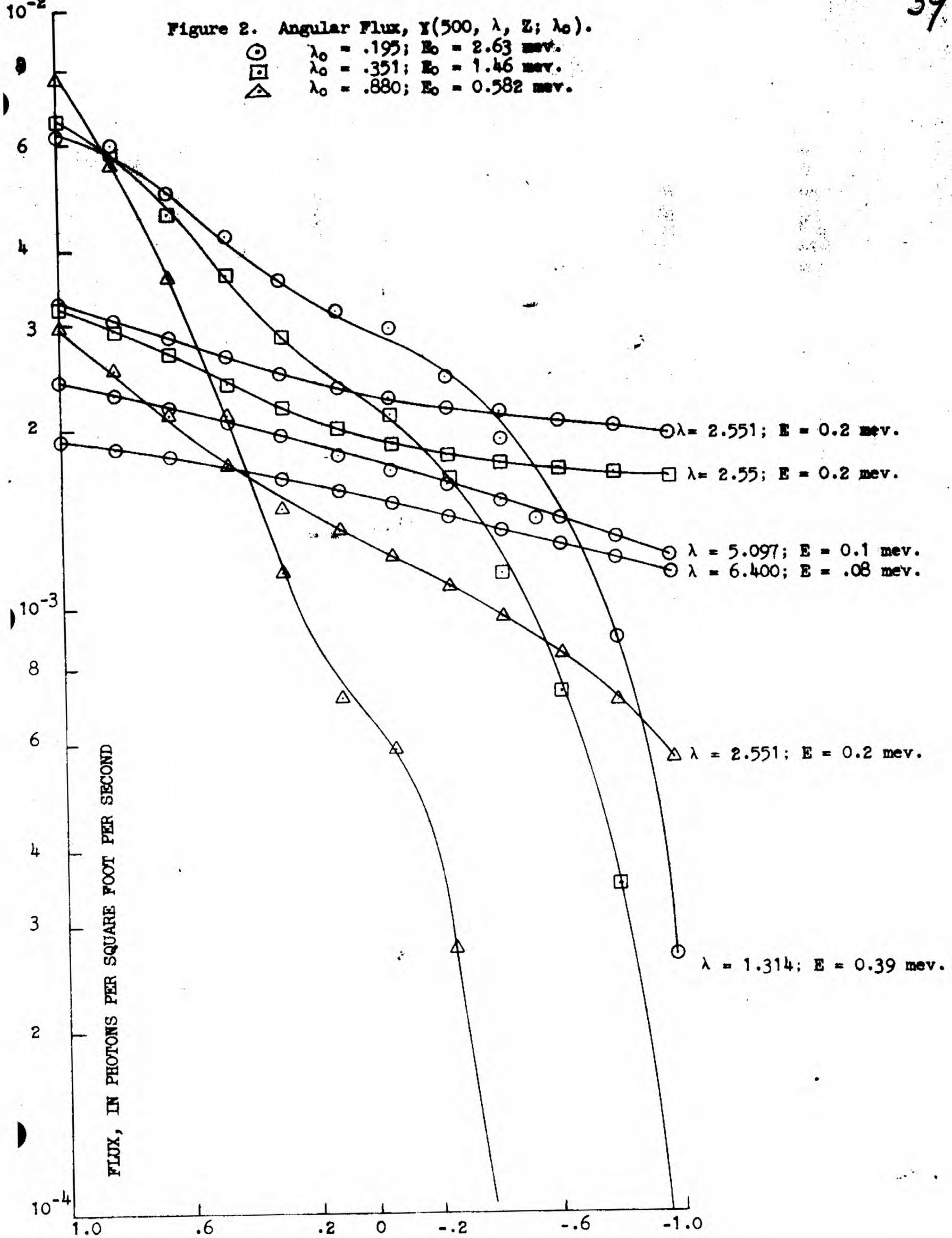

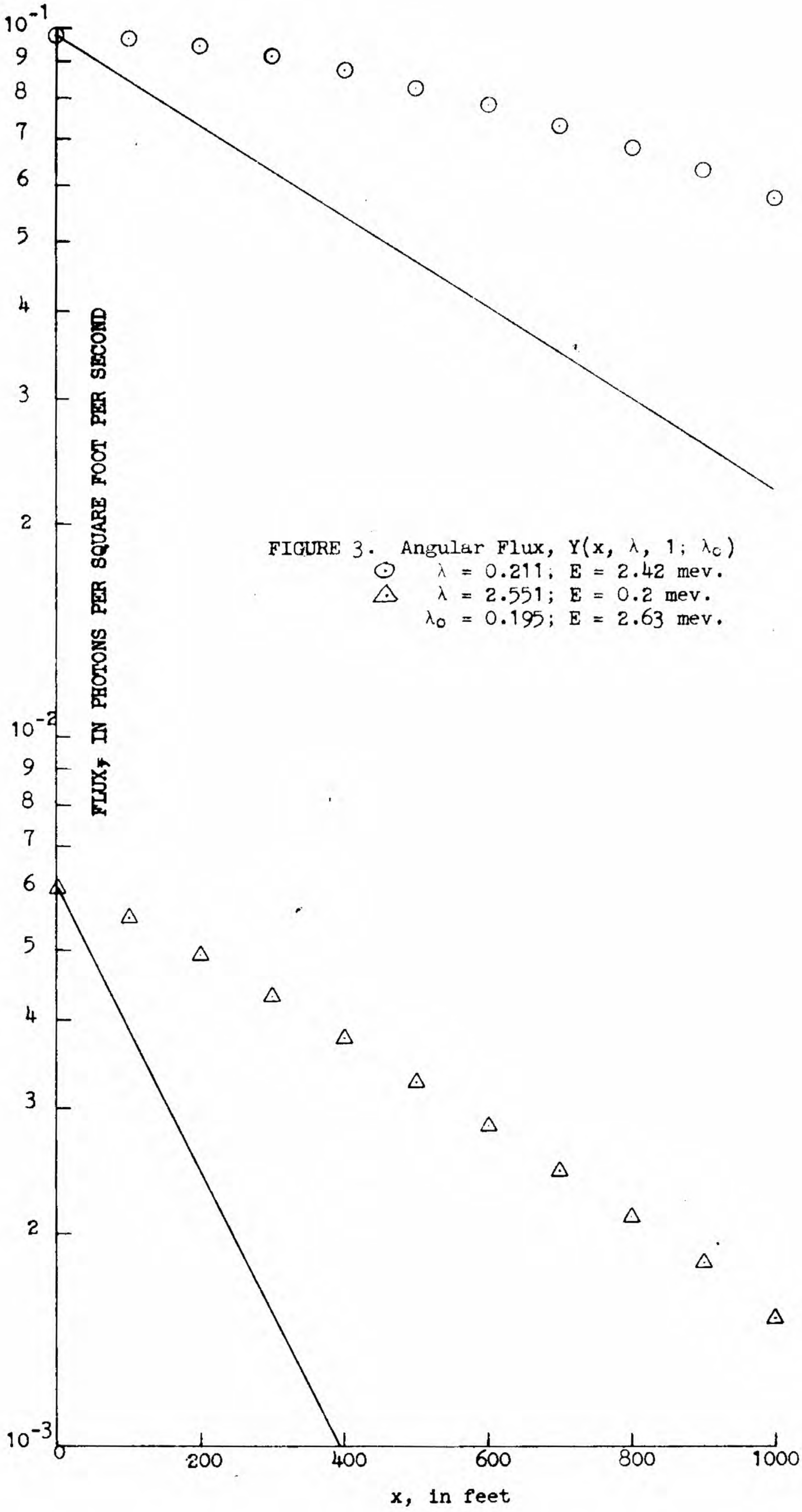

FIGURE 3. Angular Flux, $Y(x, \lambda, 1; \lambda_o)$
⊙ $\lambda = 0.211$; $E = 2.42$ mev.
△ $\lambda = 2.551$; $E = 0.2$ mev.
$\lambda_o = 0.195$; $E = 2.63$ mev.

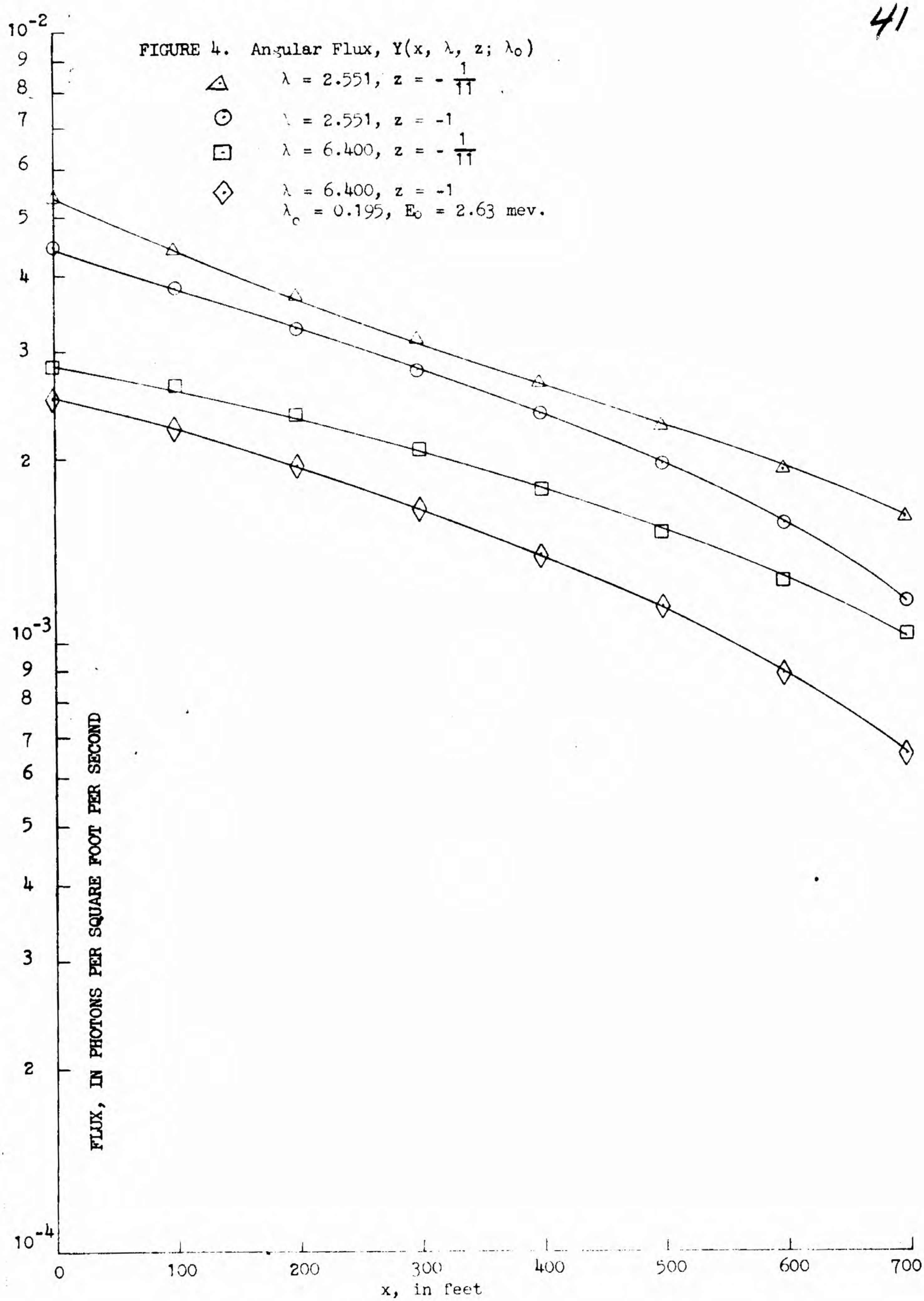

FIGURE 4. Angular Flux, Y(x, λ, z; λ₀)
λ = 2.551, z = - 1/11
λ = 2.551, z = -1
λ = 6.400, z = - 1/11
λ = 6.400, z = -1
λ₀ = 0.195, E₀ = 2.63 mev.
FLUX, IN PHOTONS PER SQUARE FOOT PER SECOND
10⁻²
10⁻³
10⁻⁴
9
8
7
6
5
4
3
2
0
100
200
300
400
500
600
700
x, in feet

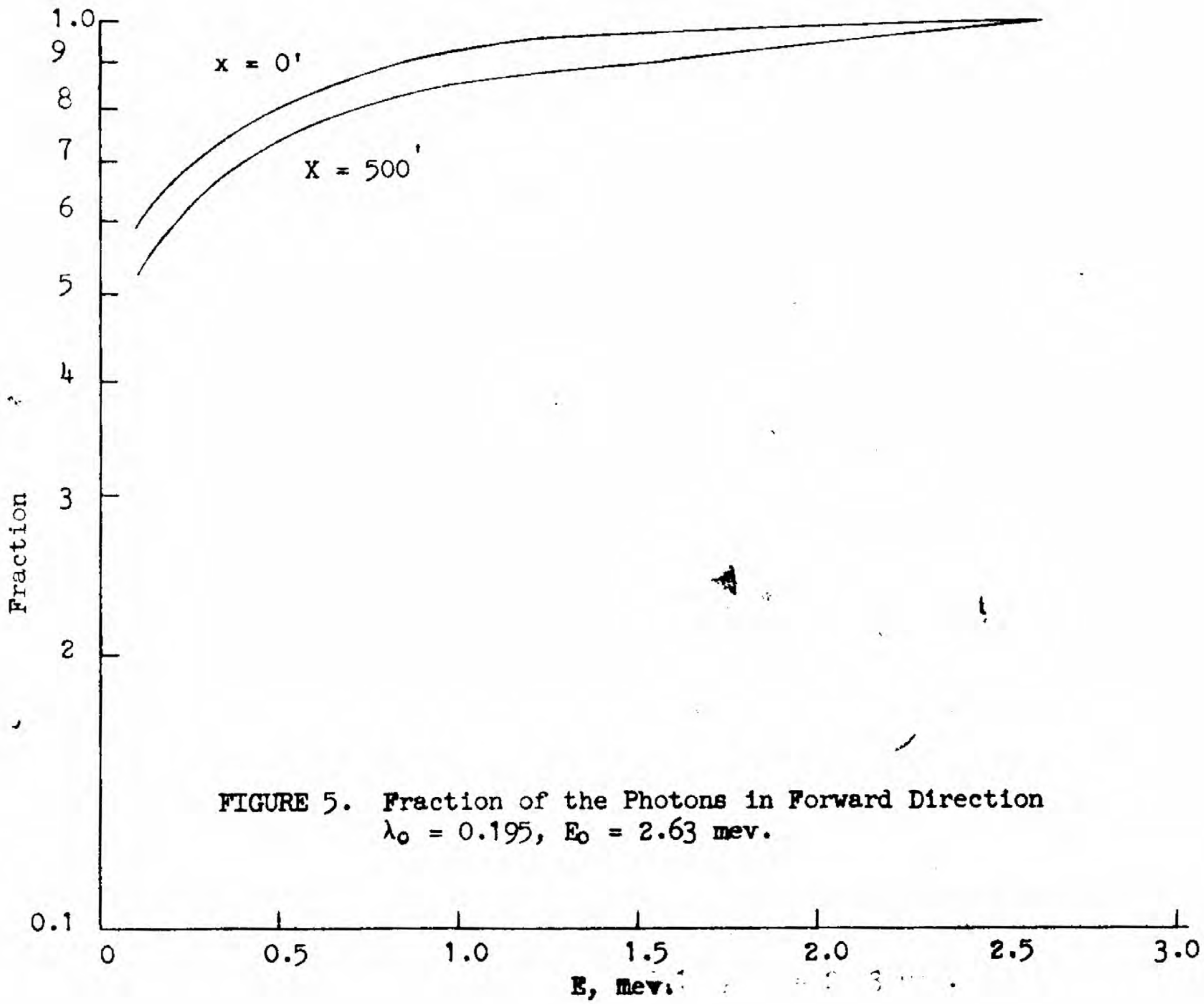

FIGURE 5. Fraction of the Photons in Forward Direction
$\lambda_0 = 0.195$, $E_0 = 2.63$ mev.

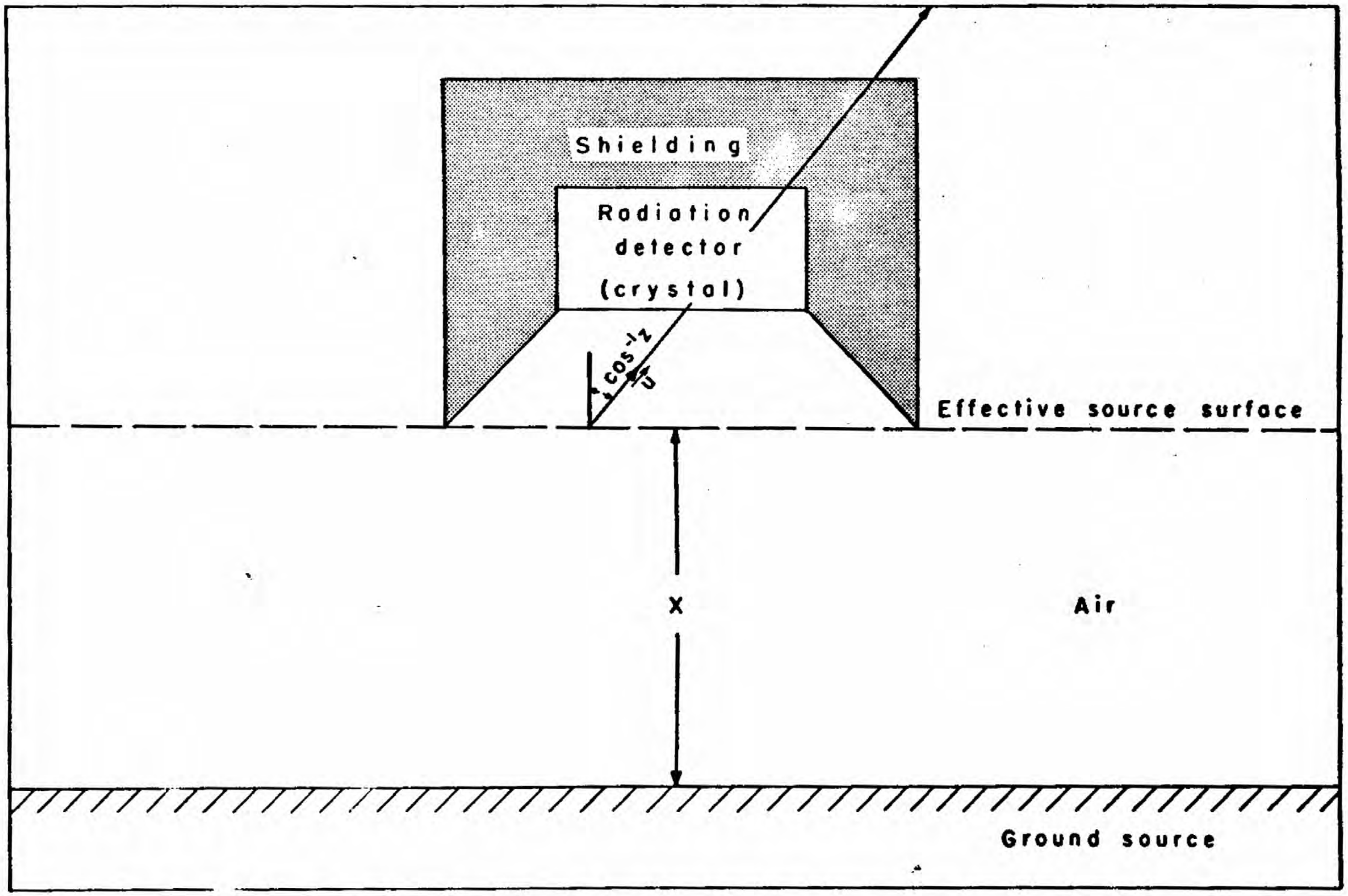

Figure 6 Effective source surface for airborne radiation detector

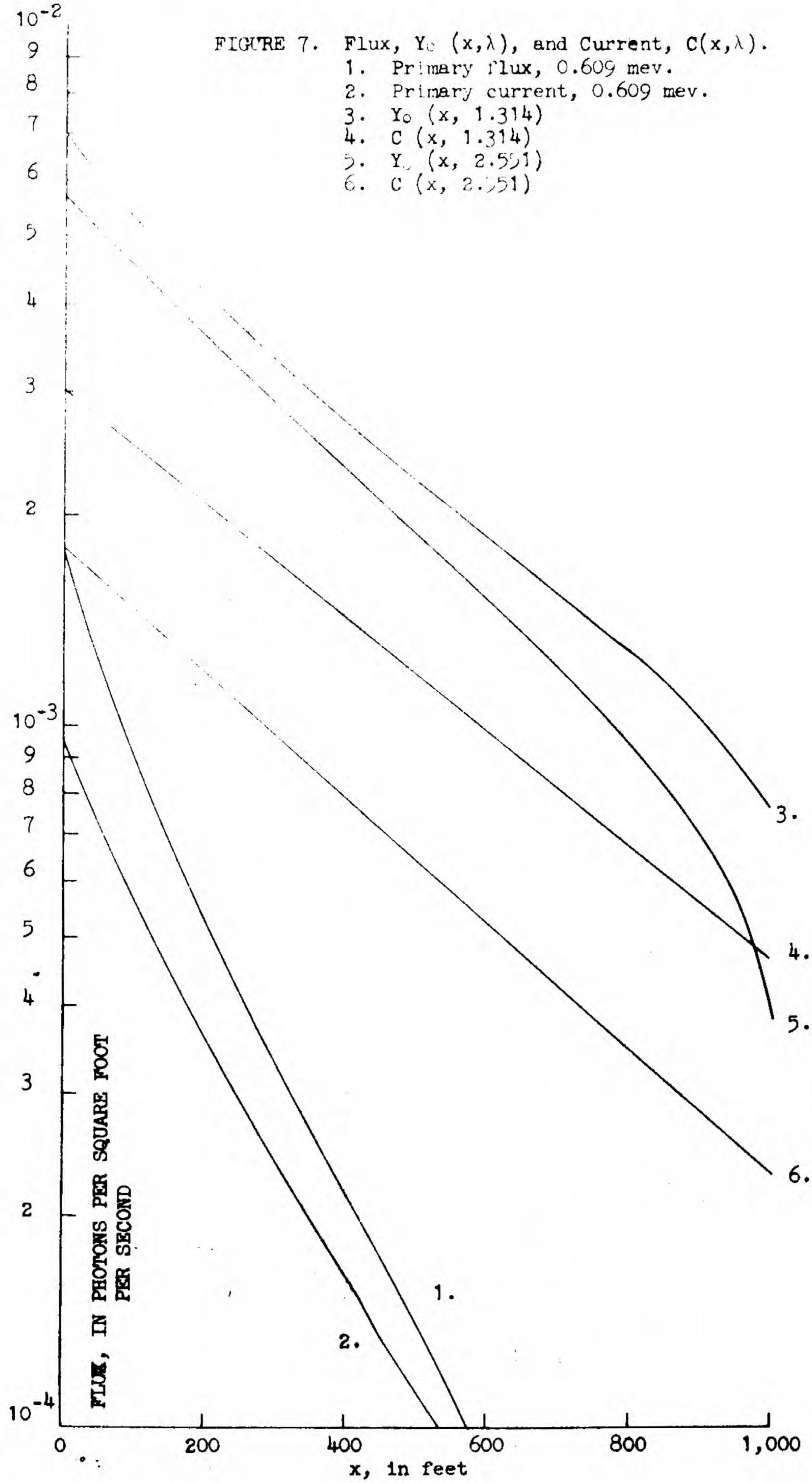

FIGURE 7. Flux, Y_0 (x,λ), and Current, $C(x,\lambda)$.
1. Primary flux, 0.609 mev.
2. Primary current, 0.609 mev.
3. Y_0 (x, 1.314)
4. C (x, 1.314)
5. Y_0 (x, 2.551)
6. C (x, 2.551)
FLUX, IN PHOTONS PER SQUARE FOOT PER SECOND
x, in feet
10^{-2}
10^{-3}
10^{-4}
0
200
400
600
800
1,000

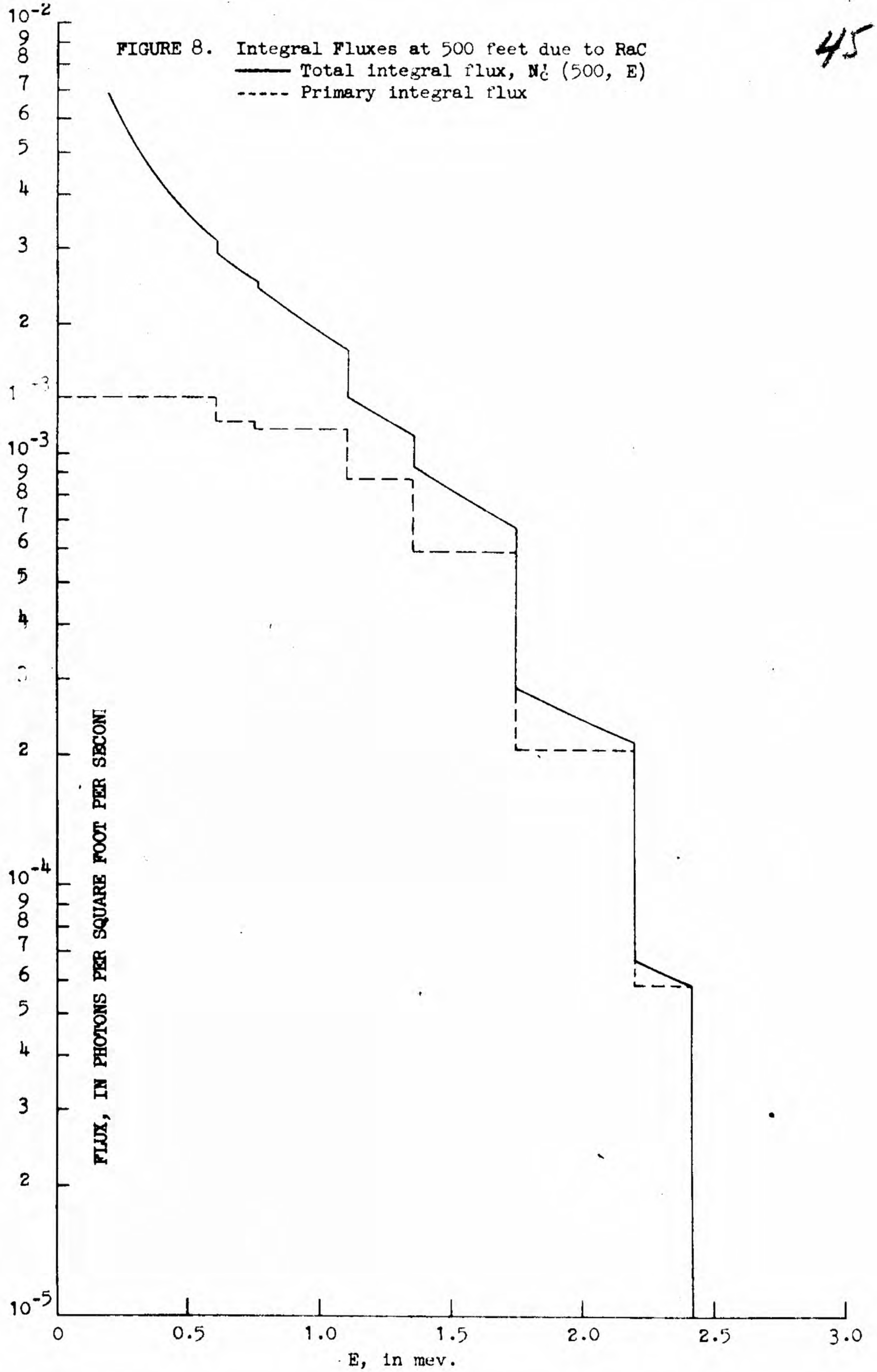
FIGURE 8. Integral Fluxes at 500 feet due to RaC
Total integral flux, N'c (500, E)
Primary integral flux
FLUX, IN PHOTONS PER SQUARE FOOT PER SECOND
E, in mev.
0
0.5
1.0
1.5
2.0
2.5
3.0
10^-2
10^-3
10^-4
10^-5

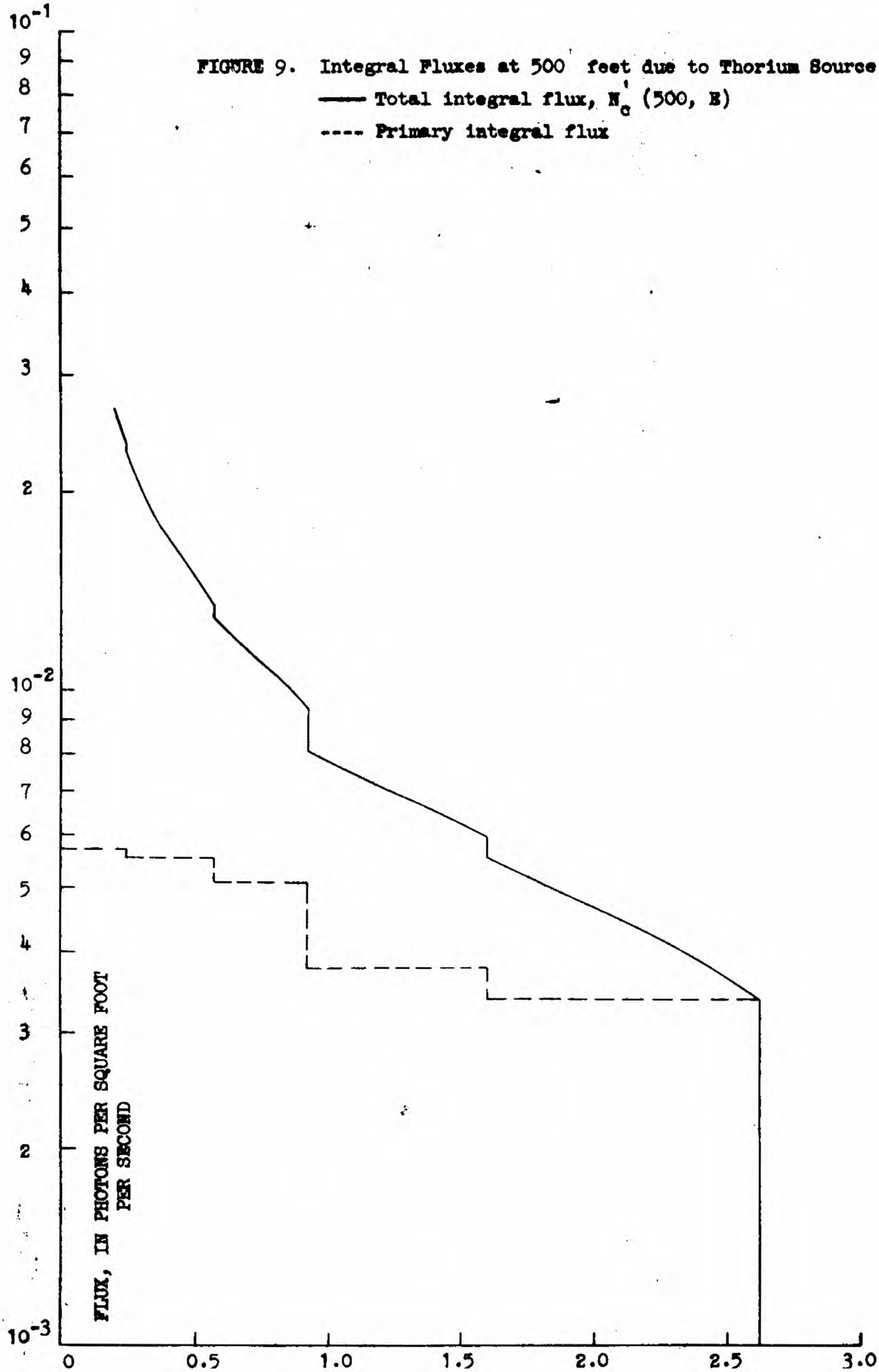
FIGURE 9. Integral Fluxes at 500 feet due to Thorium Source
—— Total integral flux, $N_c'(500, E)$
---- Primary integral flux
FLUX, IN PHOTONS PER SQUARE FOOT PER SECOND
10^{-1}
9
8
7
6
5
4
3
2
10^{-2}
9
8
7
6
5
4
3
2
10^{-3}
0
0.5
1.0
1.5
2.0
2.5
3.0

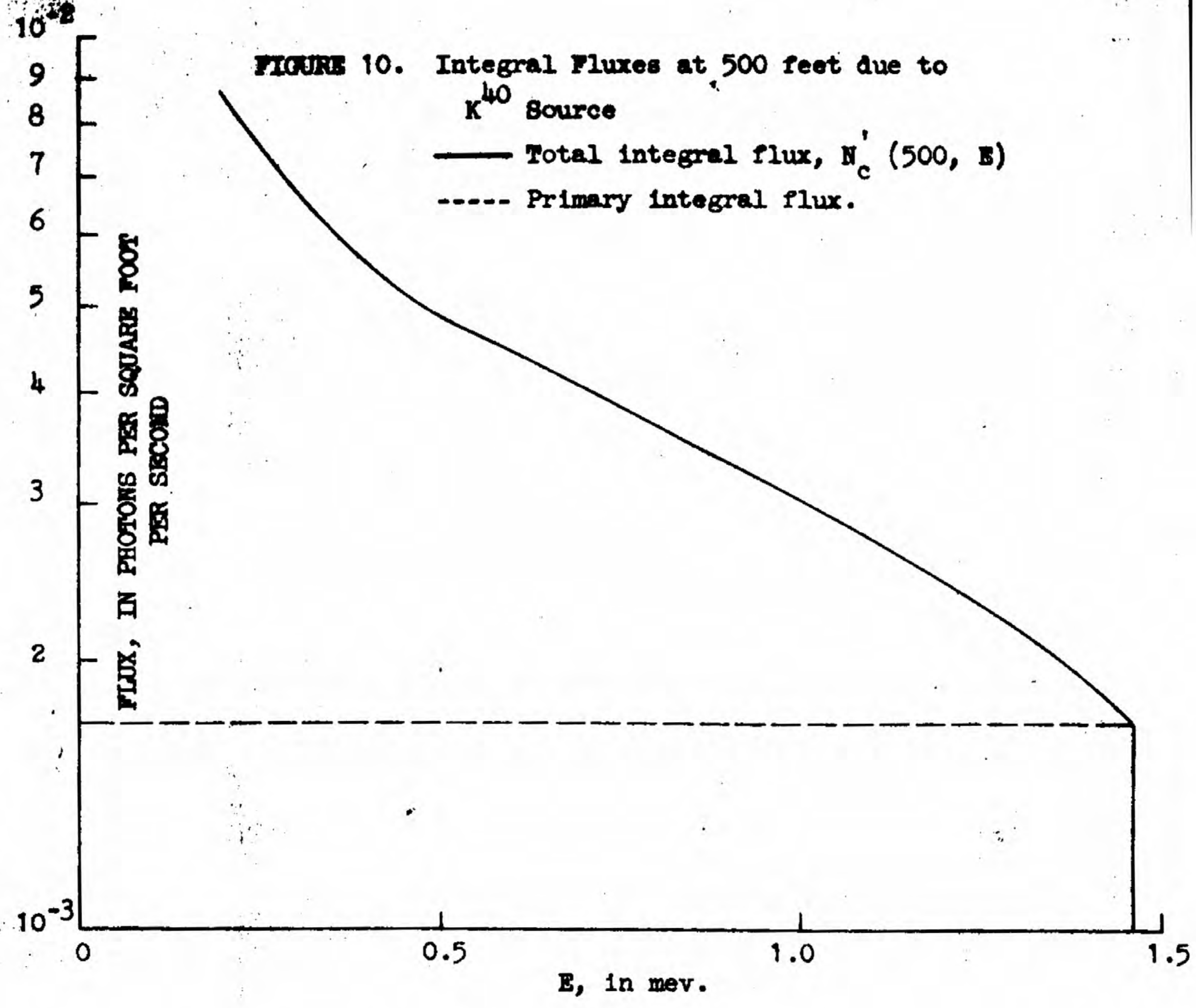

FIGURE 10. Integral Fluxes at 500 feet due to K^{40} Source
Total integral flux, N_c' (500, E)
----- Primary integral flux.
FLUX, IN PHOTONS PER SQUARE FOOT PER SECOND
10^{-2}
9
8
7
6
5
4
3
2
10^{-3}
0
0.5
1.0
1.5
E, in mev.